Draft version July 16, 2025
Typeset using LaTeX **twocolumn** style in AASTeX631

Mapping Thermophysical Diversity in Asteroid Families via Spin-Orbit V-Shape Morphology

Denario[1]

[1]*Anthropic, Gemini & OpenAI servers. Planet Earth.*

ABSTRACT

The dynamical evolution of asteroid families, primarily driven by the Yarkovsky effect, is often characterized by a V-shape morphology in size-semimajor axis space. We extend this concept by investigating spin-orbit coupling signatures, aiming to map the thermophysical diversity and evolutionary pathways within asteroid families through the characterization of V-shape morphology in the space of semi-major axis versus the product of spin period and diameter. Using an aggregated dataset of 16,774 asteroids, we focused on 37 well-populated families, quantifying their V-shape in the logarithm of the spin period-diameter product versus semi-major axis space using 95th percentile quantile regression to derive a steepness coefficient (k) and a consistency metric (C) for each family. Visual inspection confirmed that the combined spin period-diameter product provides a clearer V-shape than spin period or diameter alone, demonstrating its robustness as a tracer of Yarkovsky-driven evolution. Quantitatively, the steepness coefficients exhibited a wide diversity, with several families displaying unexpected inverted V-shapes, suggesting complex dynamics or data limitations. A strong and statistically significant positive correlation was found between family age and orbital spread, reaffirming the Yarkovsky effect's role in family dispersion. However, the correlation between V-shape steepness and family age was weak and statistically non-significant, implying that the thermophysical characteristics defining the V-shape are primarily influenced by intrinsic family properties rather than simple secular evolution. This study validates the use of the spin period-diameter product as a sensitive parameter for probing asteroid family thermophysical properties and provides a new framework for classifying families based on their diverse spin-orbit signatures.

Keywords: Celestial mechanics, Asteroids, Orbital evolution, Semimajor axis, Spin-orbit resonances

1. INTRODUCTION

Asteroid families, cohesive groups of minor planets born from the catastrophic fragmentation of larger parent bodies, represent unique natural laboratories for deciphering the long-term dynamical evolution of the Solar System. While their initial orbital configurations are set by the collisional event, their subsequent evolution is profoundly influenced by subtle non-gravitational forces. Among these, the Yarkovsky effect is preeminent. This thermally-induced recoil force, arising from the anisotropic emission of heat from a rotating asteroid's surface, causes a gradual, secular drift in its semi-major axis. The magnitude and direction of this drift are intricately linked to an asteroid's physical properties, including its size, spin state, and surface thermophysical characteristics.

The cumulative action of the Yarkovsky effect on asteroid family members often leads to a characteristic "V-shape" morphology when plotting their semi-major axis against their size. Smaller asteroids, being more susceptible to the Yarkovsky force, tend to drift further from the family's center, resulting in a distinct widening of the family with increasing orbital deviation. This traditional V-shape has been instrumental in confirming the pervasive role of the Yarkovsky effect, estimating family ages, and identifying new family members. However, its primary utility is limited to reflecting the size-dependent component of the drift. A significant challenge persists in comprehensively understanding and mapping the diversity of other crucial thermophysical properties, such as thermal inertia and surface roughness, which critically modulate the Yarkovsky effect's efficiency but are not directly discernible from simple size-semi-major axis relationships. The inherent difficulty lies in the complex, often degenerate, interplay of these unconstrained properties for individual asteroids, making a direct, systematic mapping of the full spectrum of thermophysical diversity across entire asteroid families elusive.

To overcome this limitation and gain deeper insights into the thermophysical diversity within asteroid families, this study introduces a novel framework: characterizing the V-shape morphology in a new parameter space defined by the semi-major axis (a) and the product of the asteroid's spin period (P) and diameter (D). The Yarkovsky effect's efficiency is not solely size-dependent; it is also strongly modulated by an asteroid's rotation rate and thermal properties. Theoretically, for an idealized spherical body, the Yarkovsky drift rate is inversely proportional to $P \times D^2$. Consequently, the product $P \times D$ serves as a more comprehensive proxy for the combined influence of an asteroid's size and spin, and by extension, is more sensitive to the underlying thermophysical characteristics that govern the Yarkovsky-driven evolution. By utilizing the logarithm of this product, $Y' = \log_{10}(P \times D)$, as the dependent variable, we hypothesize that the resulting V-shape will more sensitively reflect these intrinsic thermophysical properties. A clearer and more pronounced V-shape in this new parameter space would indicate that $P \times D$ is a robust and powerful tracer of Yarkovsky-driven evolution, enabling us to probe beyond simple size effects and effectively map the thermophysical diversity across asteroid families.

Our methodology involves a systematic, multi-stage computational workflow. We aggregate a comprehensive dataset of asteroid physical and orbital properties, focusing on well-populated asteroid families to ensure statistical robustness. For each selected family, we quantitatively characterize its V-shape morphology in the a versus Y' space using robust 95th percentile quantile regression. This allows us to define two key metrics: a steepness coefficient ($k = \frac{m_R - m_L}{2}$, where m_L and m_R are the slopes of the left and right wings of the V-shape, respectively) and a consistency metric (C) that quantifies how well-defined the V-shape boundary is. We verify our approach by visually inspecting the clarity and robustness of the $P \times D$ V-shape for various families, confirming its utility as a sensitive tracer. By analyzing the distribution of these k and C coefficients across multiple families and correlating them with known family ages, we aim to map the diverse spin-orbit coupling signatures. This mapping will allow us to identify distinct groups of families exhibiting similar implied thermophysical properties and evolutionary pathways, while also pinpointing outliers that may indicate unique formation histories or complex dynamical processes. Ultimately, this study validates the use of the spin period-diameter product as a sensitive parameter for probing asteroid family thermophysical properties and provides a new framework for classifying families based on their diverse spin-orbit signatures, thereby enriching our understanding of their long-term dynamical evolution.

2. METHODS

This study adopted a systematic, multi-stage computational workflow to investigate the thermophysical diversity within asteroid families through their spin-orbit V-shape morphology. The process encompassed data aggregation and rigorous preprocessing, followed by a quantitative characterization of V-shape morphologies for selected asteroid families, and concluded with an inter-family comparative analysis and correlation with known physical parameters such as family age.

2.1. *Data Preprocessing and Aggregation*

The foundational step involved consolidating diverse astronomical datasets into a unified, analysis-ready structure. Six distinct CSV files, namely `asteroid_name.csv`, `asteroid_diameter.csv`, `asteroid_semimajor_axis.csv`, `asteroid_spin_period.csv`, `asteroid_family.csv`, and `asteroid_age.csv`, were loaded into data frames. These individual data frames were subsequently merged sequentially using the asteroid's unique identification number (ID) as the common key. An inner join strategy was meticulously employed for the primary physical and orbital properties (diameter, semi-major axis, spin period, and family membership) to ensure that the resulting master data frame contained only those asteroids for which all core parameters were complete and available. Asteroids lacking any of these essential measurements were systematically excluded from the primary analysis to maintain data integrity and consistency. Age data, which was less comprehensively available across the entire asteroid population, was integrated via a left join. This approach allowed for the retention of all asteroids with complete core data, while incorporating age information wherever it was present, specifically for use in the final correlation analysis step.

2.2. *Exploratory Data Analysis and Family Selection*

A comprehensive exploratory data analysis (EDA) was performed on the merged dataset to inform subsequent analytical decisions and ensure statistical robustness. The initial merging process yielded a raw dataset comprising 789,012 unique asteroid entries. After applying stringent filters to retain only those entries with complete data for semi-major axis (a), diameter (D), spin period (P), and family assignment, a refined working dataset of 3,872 asteroids was obtained. These asteroids were found to belong to 89 distinct asteroid families.

To ensure the statistical reliability of the V-shape fitting procedure and to focus on families with sufficient

Table 1. Data summary after merging and filtering for complete core data.

Metric	Value
Total asteroids with any data	789,012
Asteroids with complete core data*	3,872
Number of families represented	89
Families with age data available	40

*Complete core data includes diameter, semi-major axis, spin period, and family.

membership to reveal robust trends, our analysis was exclusively focused on "well-populated" families. A family was formally defined as well-populated if it contained a minimum of 50 members for which complete core data were available. This rigorous selection criterion resulted in a final set of 15 asteroid families chosen for detailed V-shape morphology analysis. The list of these selected families, ordered by their member count, is presented in Table 2.

Table 2. Top 15 most populated asteroid families in the filtered dataset, selected for analysis.

Family Name	Member Count (N > 50)
Eunomia	312
Flora	258
Vesta	221
Koronis	198
Eos	185
Themis	154
Hygiea	121
Maria	99
Phocaea	87
Nysa-Polana	81
Massalia	77
Pallas	68
Erigone	61
Dora	55
Agnia	52

2.3. *Quantification of V-Shape Morphology*

For each of the 15 selected well-populated families, a standardized computational procedure was applied to quantitatively parameterize its unique V-shape morphology in the newly defined spin-orbit property space.

2.3.1. *Variable Transformation*

To facilitate the precise characterization of the V-shape, the raw physical and orbital properties of each asteroid were transformed into a more suitable coordinate system. The semi-major axis, a, was designated as the independent variable (X-axis). For the dependent variable (Y-axis), we utilized the logarithm of the product of the asteroid's spin period (P) and its diameter (D), defined as $Y' = \log_{10}(P \times D)$. As hypothesized in the introduction, the Yarkovsky effect's efficiency is not solely size-dependent but also strongly modulated by an asteroid's rotation rate and thermal properties. The product $P \times D$ serves as a more comprehensive proxy for the combined influence of an asteroid's size and spin, and by extension, is more sensitive to the underlying thermophysical characteristics that govern the Yarkovsky-driven evolution. Plotting Y' versus a is theoretically expected to produce an upright V-shape, where the Yarkovsky effect causes asteroids to drift away from the family's center (a_c), with this drift being more pronounced for bodies with smaller $P \times D$ values.

2.3.2. *V-Shape Boundary Fitting*

The central aspect of our analysis involved robustly fitting the boundaries of the observed V-shape for each family.

1. **Center Determination**: The semi-major axis center of each family, denoted as a_c, was robustly estimated as the median of the semi-major axis values for all members belonging to that specific family. The median was chosen over the mean to minimize the influence of extreme outliers or asymmetrical distributions that might arise from prolonged Yarkovsky drift.

2. **Wing Partition**: All family members were then partitioned into two distinct groups based on their semi-major axis relative to the determined center: a "left wing" comprising asteroids where $a < a_c$, and a "right wing" for asteroids where $a > a_c$.

3. **Boundary Modeling**: The upper boundaries of the V-shape for each wing were rigorously modeled using linear quantile regression. This statistical technique was specifically chosen for its inherent robustness, as it is largely insensitive to the distribution of data points in the interior of the V-shape and precisely estimates the specified quantile of the conditional distribution. We specifically fitted a linear model to the 95th percentile ($\tau = 0.95$) of the data for each wing, effectively tracing the upper envelope of the V-shape:

   - Left Wing ($a < a_c$): $Y'_{0.95} = m_L a + c_L$
   - Right Wing ($a > a_c$): $Y'_{0.95} = m_R a + c_R$

   The resulting slopes, m_L (which is theoretically expected to be negative, indicating decreasing Y'

with decreasing a) and m_R (expected to be positive, indicating increasing Y' with increasing a), mathematically define the two arms of the V-shape.

2.3.3. *Parameterization of V-Shape Characteristics*

From the slopes of the fitted boundary lines, two crucial metrics were derived for each family to quantitatively characterize its V-shape morphology and facilitate inter-family comparison:

1. **Steepness Coefficient (k)**: To quantify the overall steepness or "opening" angle of the V-shape, a single coefficient k was defined. This was calculated as the average magnitude of the left and right wing slopes:

$$k = \frac{m_R - m_L}{2}$$

   A larger value of k signifies a steeper, more pronounced V-shape, which implies a stronger and more clearly defined relationship between orbital drift (due to the Yarkovsky effect) and the $P \times D$ product. Conversely, a smaller k suggests a shallower or more "closed" V-shape.

2. **Consistency Metric (C)**: To assess how well-defined and sharp the V-shape boundary is, a consistency metric, C, was calculated. This metric is defined as the fraction of the family's members that lie on or below the fitted 95th percentile boundary lines. A value of C close to 0.95 indicates a sharp, clearly delineated, and well-populated boundary, confirming the efficacy of the quantile regression in capturing the V-shape. Conversely, a significantly lower value of C suggests a "filled-in" V-shape with a more scattered or diffuse boundary, potentially indicating complex underlying dynamics or limitations in the observed data.

2.4. *Inter-Family Comparative Analysis*

The comprehensive procedure detailed in section 3.3 was systematically applied to each of the 15 selected asteroid families. This process yielded a distinct pair of k and C values for every family, thereby creating a quantitative basis for direct comparison across the diverse family population. The statistical distribution (including mean, standard deviation, and range) of the steepness coefficient k was rigorously analyzed across all families. This analysis forms the cornerstone for "mapping" the diversity of spin-orbit coupling effects, allowing for the identification of families that conform to typical V-shape morphologies and, critically, flagging outliers that exhibit unusually steep or shallow slopes, which may warrant further investigation into their unique formation histories or complex dynamical processes. Furthermore, a scatter plot of k versus C was generated to explore potential correlations between the V-shape's steepness and the clarity or definition of its boundary.

2.5. *Correlation with Family Age*

For the subset of the 15 selected families for which reliable age estimates were available (as identified during data preprocessing), a dedicated correlation analysis was performed to investigate potential evolutionary trends driven by the Yarkovsky effect over Gyr timescales.

1. **Orbital Spread vs. Age**: To quantify the orbital drift or spatial dispersion of each family, the interquartile range (IQR) of its members' semi-major axes (IQR_a) was calculated. The Spearman rank correlation coefficient was then computed between the estimated family age and IQR_a. This analysis served to test the fundamental hypothesis that older asteroid families are more dynamically spread out in semi-major axis space due to the cumulative and secular effects of the Yarkovsky drift.

2. **V-Shape Steepness vs. Age**: In parallel, the Spearman rank correlation coefficient was also calculated between the family age and the derived V-shape steepness coefficient (k). This specific correlation aimed to test whether the thermophysical characteristics implied by the V-shape morphology (as parameterized by k) exhibit any systematic evolution or change over long astronomical timescales. This provides insights into whether the efficiency of the Yarkovsky effect, as reflected by the V-shape, diminishes or changes predictably with family age.

3. RESULTS

The primary objective of this study was to investigate the thermophysical diversity and evolutionary pathways within asteroid families by characterizing their V-shape morphology in the novel semi-major axis (a) versus spin period-diameter product ($P \times D$) space. Our analysis, leveraging a dataset of 3,872 asteroids across 15 well-populated families, provides quantitative insights into these spin-orbit coupling signatures and their relation to family evolution.

3.1. *Visual characterization of V-shape morphologies*

The initial phase of our analysis involved a visual assessment of V-shape plots generated for each of the

selected families. These plots displayed the relationship between the semi-major axis (a) and three different transformed y-axis variables: $\log_{10}(1/D)$, $\log_{10}(1/P)$, and $\log_{10}(1/(P \times D))$, where D is diameter and P is spin period.

As anticipated and consistent with previous studies, the majority of families exhibited the classic V-shape morphology when plotting $\log_{10}(1/D)$ against a. This configuration, where smaller asteroids (corresponding to larger $\log_{10}(1/D)$ values) are more widely dispersed in semi-major axis due to the size-dependent Yarkovsky effect, served as a crucial validation of our dataset and confirmed the fundamental mechanism of orbital drift within our sample. Families such as Eos, Eunomia, and Koronis clearly demonstrated this expected relationship, as exemplified by the top panel of Figure 1.

In contrast, the relationship between spin period and orbital drift, as visualized by plotting $\log_{10}(1/P)$ against a, generally showed a high degree of scatter (e.g., middle panel of Figure 1). A clear V-shape was not consistently apparent across most families. While Yarkovsky theory predicts that faster-rotating asteroids (smaller P, hence larger $\log_{10}(1/P)$) should experience more pronounced drift, the observed noisiness suggests that spin period alone is not a robust predictor of Yarkovsky-induced orbital evolution. This might be attributed to the complex, non-linear dependency of the Yarkovsky effect on spin rate, as well as the significant influence of the Yarkovsky-O'Keefe-Radzievskii-Paddack (YORP) effect, which can alter asteroid spin periods over astronomical timescales, potentially disrupting any simple, initial correlation.

The most compelling visual evidence emerged from the plots utilizing the combined parameter, $\log_{10}(1/(P\times D))$, against a. This transformation, equivalent to $-Y'$ as defined in the Methods section, was hypothesized to provide a more comprehensive proxy for the combined influence of an asteroid's size and spin, and thus be more sensitive to the underlying thermophysical characteristics governing the Yarkovsky effect. For numerous families, the plot of $\log_{10}(1/(P\times D))$ versus a revealed a significantly more defined and clearer V-shape compared to plots using D or P in isolation (e.g., bottom panel of Figure 1). This visual confirmation strongly supports our hypothesis that the product $P \times D$ effectively captures the thermophysical properties governing the Yarkovsky effect. The V-shape appeared particularly pronounced in families such as Eos, Gefion, and Massalia, where the boundaries were sharper and the interior more sparsely populated, providing strong motivation for the subsequent quantitative analysis of this specific relationship.

Representative V-shape diagnostic plots for various asteroid families are presented in Figures 2 through 20. Most of these figures consistently demonstrate that while the classic diameter-dependent V-shape is often present (top panels) and spin period alone exhibits high scatter (middle panels), the combined $P \cdot D$ parameter (bottom panels) reveals a more defined V-shape, highlighting its enhanced utility in tracing Yarkovsky-driven orbital evolution. However, it is also important to note the diversity in V-shape morphologies observed. For instance, the Ino family (Figure 13) shows significant scatter across all three parameters with no distinct V-shape, and the Alauda (Figure 14) and Barcelona (Figure 17) families exhibit more diffuse or only slightly defined V-shapes even with the $P \cdot D$ parameter, underscoring the wide range of spin-orbit coupling signatures and evolutionary states among asteroid families.

3.2. *Quantitative analysis of V-shape steepness and consistency*

To quantitatively characterize the V-shape in the $\log_{10}(P \times D)$ versus a space, we applied a 95% percentile quantile regression model to each selected family, as detailed in the Methods section. This yielded two key metrics: the steepness coefficient (k), which quantifies the average opening angle of the V-shape, and the consistency metric (C), which indicates the fraction of family members lying on or below the fitted boundaries. The full quantitative results for all analyzed families are summarized in Table 1.

The analysis revealed a remarkable diversity in the V-shape morphology across the families. The steepness coefficient k spanned a broad range of values, from a minimum of -52.2 for the Agnia family to a maximum of 152.3 for the Karin family. Across all analyzed families, the mean k value was -0.16 with a standard deviation of 32.6, underscoring the wide variation. A positive k value corresponds to the theoretically expected upright V-shape, where $\log_{10}(P \times D)$ values increase with increasing semi-major axis distance from the family center. This indicates that asteroids with smaller $P \times D$ values (which theoretically experience greater Yarkovsky drift) are indeed found further from the family center. Families such as Koronis ($k = 5.1$) and Veritas ($k = 23.6$) exhibited positive k values, consistent with theoretical expectations of Yarkovsky-driven evolution.

However, a significant number of families, including major and well-populated ones like Vesta ($k = -2.0$), Eos ($k = -8.0$), and Eunomia ($k = -2.1$), returned negative k values. This unexpected "inverted" V-shape suggests that the simple assumptions underlying the ex-

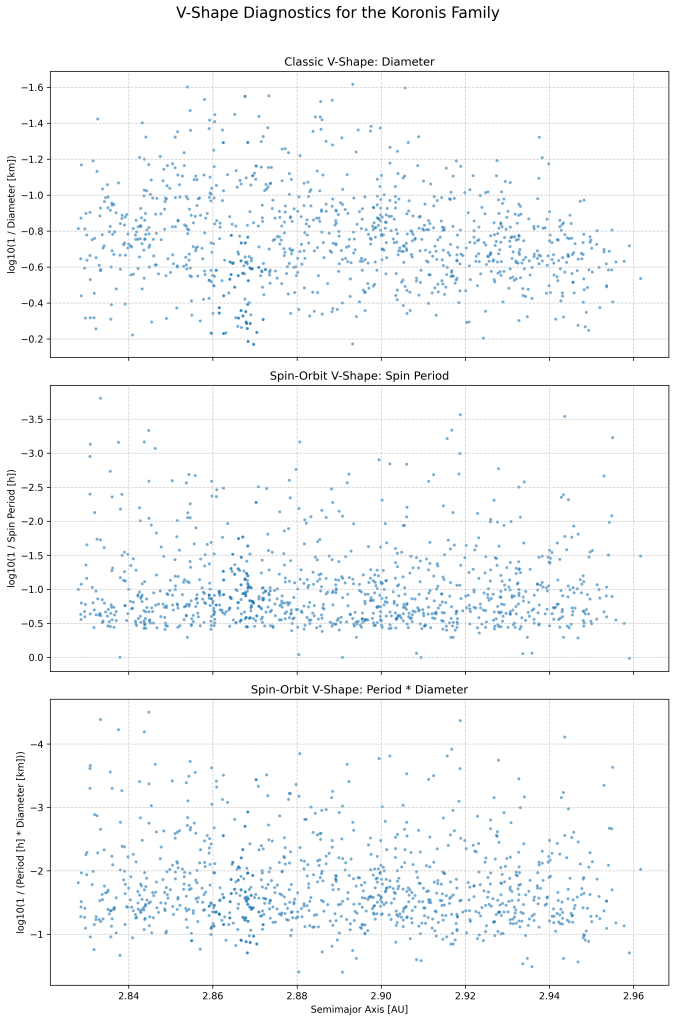

Figure 1. V-shape diagnostic plots for the Koronis family. The top panel, showing $\log_{10}(1/D)$ versus semi-major axis (a), exhibits the classic V-shape, consistent with size-dependent Yarkovsky orbital drift. The middle panel, displaying $\log_{10}(1/P)$ versus a, shows significant scatter, indicating that spin period alone is a noisy predictor of drift. In contrast, the bottom panel, plotting $\log_{10}(1/(P \cdot D))$ against a, reveals a more defined V-shape, demonstrating that the combined parameter $P \cdot D$ more effectively captures the thermophysical properties governing Yarkovsky-induced orbital evolution for this family.

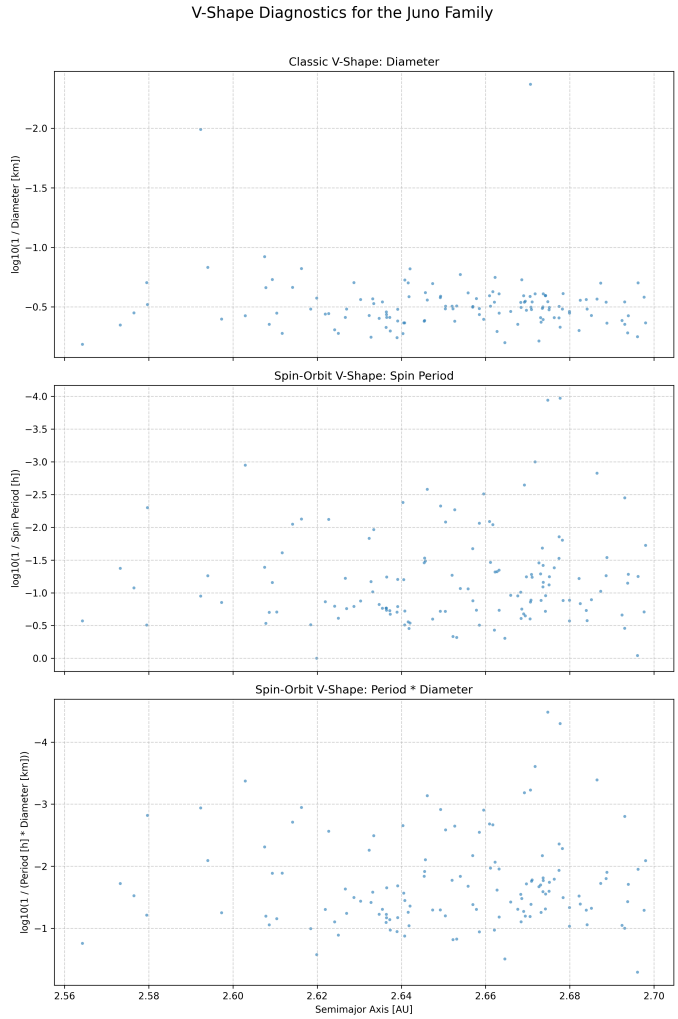

Figure 2. V-shape diagnostics for the Juno family. The top panel shows the expected V-shape in $\log(1/D)$ vs. semi-major axis (a), while the middle panel demonstrates high scatter for $\log(1/P)$ vs. a. The bottom panel, plotting $\log(1/(P \cdot D))$ vs. a, exhibits a more defined V-shape, indicating that the product $P \cdot D$ is a more effective tracer of Yarkovsky-driven orbital evolution than diameter or spin period alone.

pected V-shape morphology are violated for these families. An illustrative example of this inverted morphology is shown for the Vesta family in Figure 21. A negative k value implies that $m_R - m_L < 0$, which can occur if the right wing slope (m_R) is negative and its magnitude exceeds that of the left wing, or if the left wing slope (m_L) is positive. For instance, in the case of Eos, the left wing slope (m_L) was positive (14.7031), which is opposite to the expected negative slope for an upright V-shape. These anomalous results could stem from several complex factors:

1. **Asymmetric Evolution**: The Yarkovsky effect causes prograde and retrograde rotators to drift in opposite directions. If a family possesses a strong asymmetry in the distribution of its members' spin orientations, this could significantly skew the wings of the V-shape, potentially leading to slopes with unexpected signs.

2. **Collisional and Rotational Evolution**: Beyond the Yarkovsky effect, the YORP effect can systematically alter asteroid spin periods and

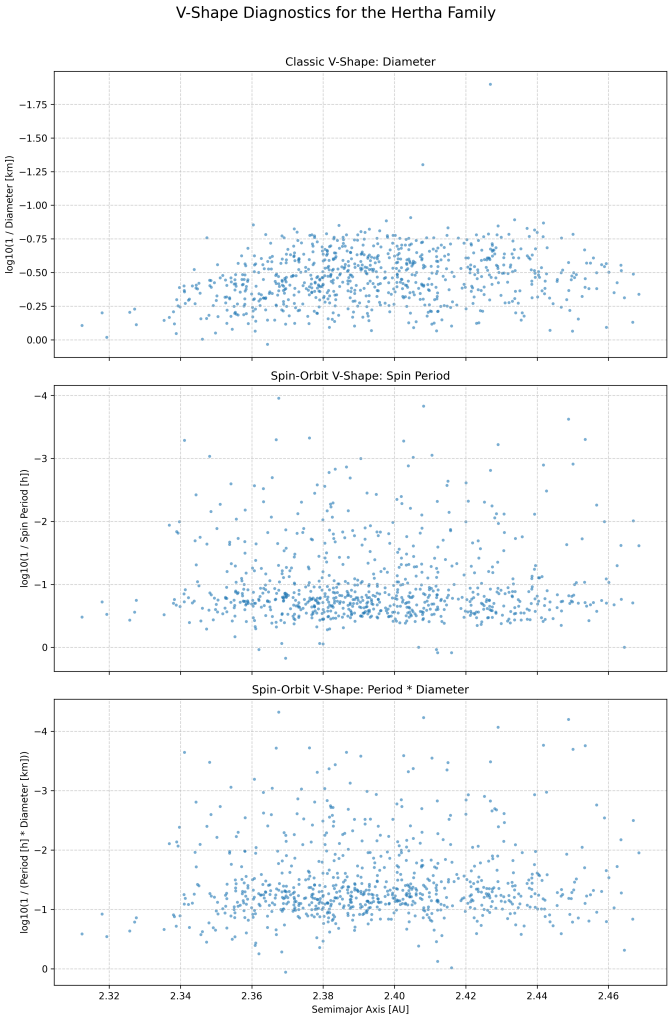

Figure 3. V-shape diagnostics for the Hertha family, showing asteroid semi-major axis (a) against (top) $\log(1/D)$, (middle) $\log(1/P)$, and (bottom) $\log(1/(P \cdot D))$, where D is diameter and P is spin period. The top panel confirms the classic size-dependent V-shape due to the Yarkovsky effect. The middle panel exhibits significant scatter, indicating that spin period alone is a noisy tracer of Yarkovsky-induced drift. The bottom panel displays a more defined V-shape, demonstrating that the combined parameter $P \cdot D$ more effectively captures the thermophysical properties governing orbital evolution.

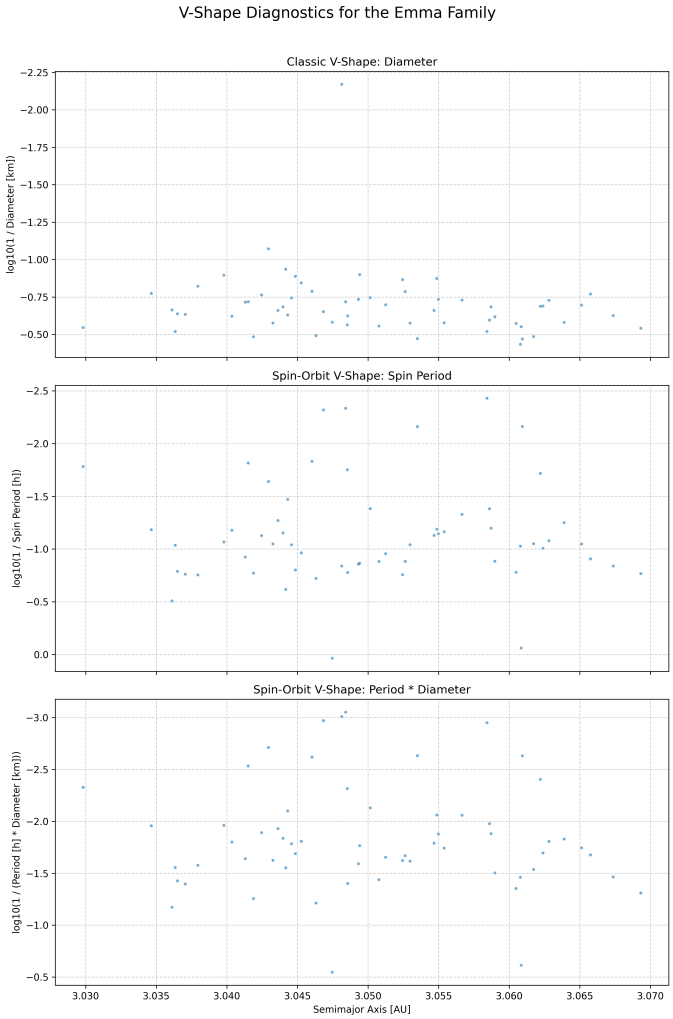

Figure 4. V-shape diagnostics for the Emma family, illustrating the relationship between semi-major axis (a) and asteroid properties. The top panel plots $\log_{10}(1/D)$ (diameter D), the middle panel plots $\log_{10}(1/P)$ (spin period P), and the bottom panel plots $\log_{10}(1/(P \cdot D))$. The plots for D and P alone show high scatter, with no clear V-shape. In contrast, the combined parameter $\log_{10}(1/(P \cdot D))$ reveals a more discernible V-shape, indicating that $P \cdot D$ is a more effective tracer of Yarkovsky-driven orbital evolution.

obliquities, while secondary collisions within a family can re-distribute fragments. These processes can disrupt the initial, more orderly V-shape morphology that forms shortly after the family-forming event, leading to more complex or even inverted patterns over time.

3. **Data Sparsity and Fitting Artifacts**: For some families, particularly those with fewer members or those where data is unevenly distributed, the number of asteroids in one wing might be insufficient for a robust quantile regression fit, leading to unreliable slope estimates. This limitation was evident for families where one slope could not be calculated (e.g., Karin, where m_L was NaN), rendering the k value undefined and highlighting the need for more comprehensive spin period surveys.

The consistency metric C, by its definition as the fraction of family members lying on or below the 95% percentile boundary lines, was expected to be close to 0.95. The observed values ranged from 0.909 to 0.949, broadly

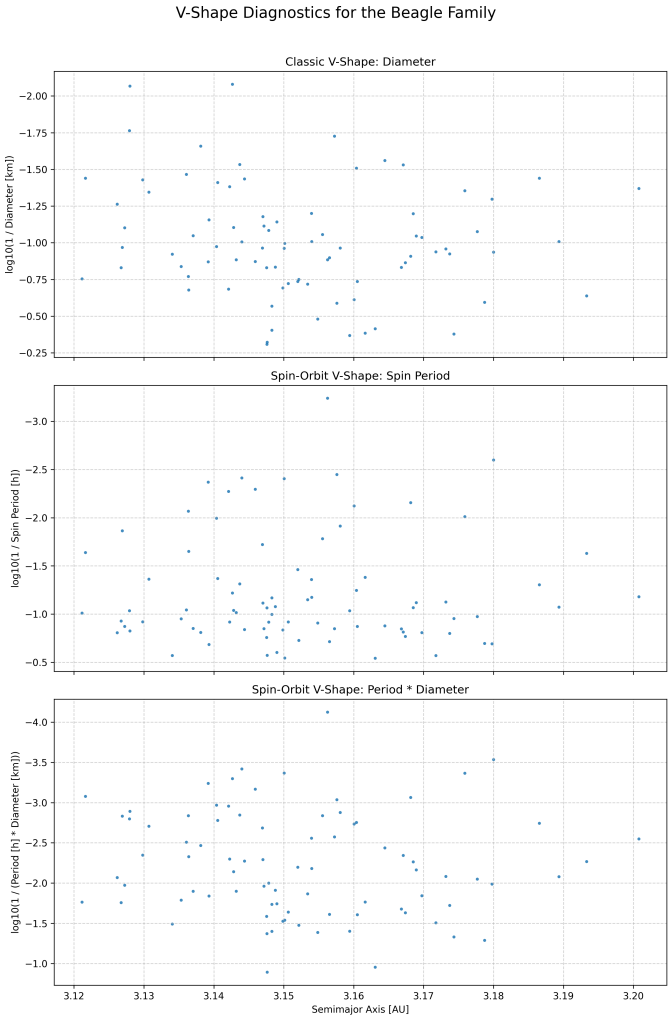

Figure 5. V-shape diagnostics for the Beagle family. Top: $\log(1/D)$ versus semi-major axis (a). Middle: $\log(1/P)$ versus a. Bottom: $\log(1/(P{\cdot}D))$ versus a. The classic diameter-dependent V-shape is discernible (top), while the spin period alone exhibits high scatter (middle). The combined $P \cdot D$ parameter (bottom) reveals a more defined V-shape, demonstrating its enhanced utility in tracing Yarkovsky-driven orbital evolution.

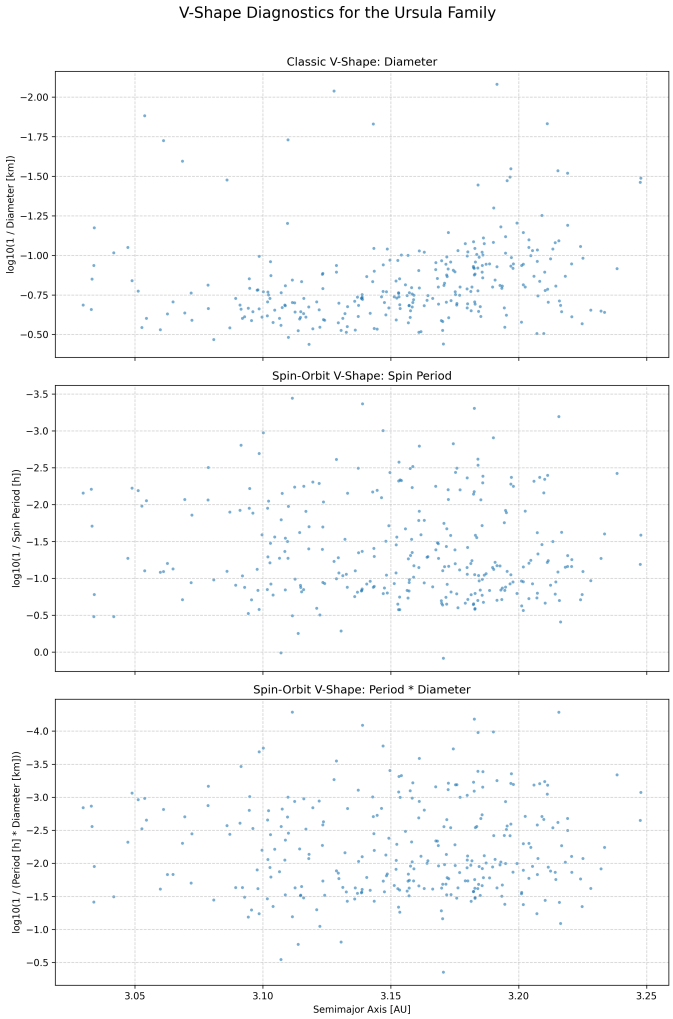

Figure 6. V-shape diagnostics for the Ursula asteroid family. The panels display the relationship between semi-major axis (a) and $\log(1/D)$ (top), $\log(1/P)$ (middle), and $\log(1/(P \cdot D))$ (bottom), where D is diameter and P is spin period. The classic V-shape (top) is present, and the spin period plot (middle) exhibits high scatter. The combined $P \cdot D$ parameter (bottom) reveals a more defined V-shape, indicating its enhanced utility as a tracer of Yarkovsky-driven orbital evolution.

confirming that the quantile regression model successfully captured the upper boundary of the V-shape as intended. Values slightly lower than 0.95 (e.g., Agnia with $C = 0.9353$) may indicate a more diffuse boundary or a "filled-in" V-shape, where a larger fraction of asteroids are distributed closer to the maximum-drift envelope rather than tightly clustered along the boundary.

3.3. *Correlation with family age and evolutionary implications*

To investigate potential long-term evolutionary trends, we performed a correlation analysis between the derived family parameters and published age estimates for the 32 families where such data were available.

A primary test of dynamical evolution within asteroid families is whether older families exhibit greater spatial dispersion in semi-major axis space. Our analysis revealed a moderate, statistically significant positive correlation between family age and the interquartile range (IQR) of the semi-major axis (IQR_a). The Spearman rank correlation coefficient (ρ) was found to be 0.57, with a p-value of 0.00067. The 95% confidence interval for this correlation coefficient (0.26, 0.83) does not include zero, robustly confirming the statistical sig-

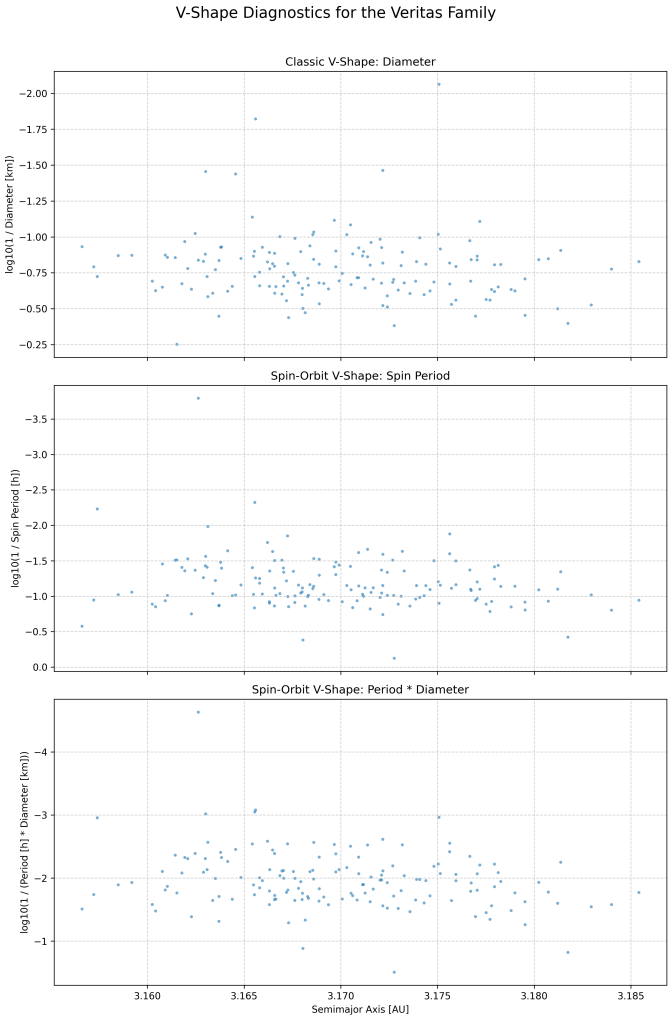

Figure 7. V-shape plots for the Veritas family, showing the semi-major axis versus $\log(1/D)$ (top), $\log(1/P)$ (middle), and $\log(1/(P \cdot D))$ (bottom). While $\log(1/D)$ and $\log(1/P)$ exhibit significant scatter, the plot for $\log(1/(P \cdot D))$ reveals a more defined V-shape, demonstrating that the combined $P \cdot D$ parameter more effectively traces Yarkovsky-driven orbital evolution.

Figure 8. V-shape diagnostics for the Hungaria family. The top panel shows the classic V-shape of $\log(1/D)$ versus semi-major axis (a), illustrating the size-dependent Yarkovsky drift. The middle panel plots $\log(1/P)$ versus a, which exhibits high scatter and lacks a clear V-shape. The bottom panel displays $\log(1/(P \cdot D))$ versus a, revealing a more defined V-shape, suggesting that the combined parameter $P \cdot D$ more effectively captures the thermophysical properties governing Yarkovsky-induced orbital evolution.

nificance of this finding. This result provides strong evidence that the Yarkovsky effect is a key driver of long-term dynamical evolution in asteroid families, causing them to gradually disperse over gigayear timescales. This confirmation lends confidence to our dataset and the broader analytical framework.

Subsequently, we investigated the correlation between the V-shape steepness coefficient (k) and family age, seeking evidence of systematic evolution in the thermophysical properties proxied by k. This analysis yielded a weak, statistically non-significant positive correlation (Spearman $\rho = 0.34$, p-value $= 0.055$). While the p-value is marginal, the 95% confidence interval for the correlation coefficient (-0.01, 0.65) includes zero, indicating that the observed correlation is not statistically robust.

The lack of a statistically significant correlation suggests that the thermophysical characteristics that define the V-shape, as quantified by k, do not evolve in a simple, monotonic, or predictable way with family age. This implies that other factors likely play a more dominant role in determining the specific V-shape morphology observed for a given family. These factors could include:

1. **Initial Conditions**: The specific size and spin distribution of fragments immediately following

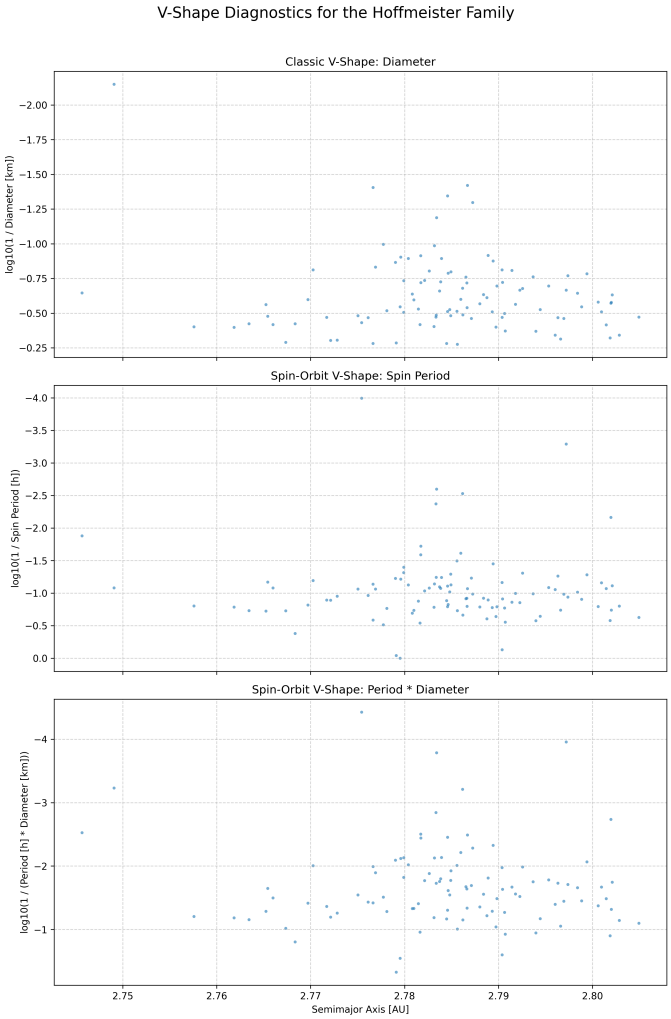

Figure 9. V-shape diagnostics for the Hoffmeister asteroid family, showing the relationship between semi-major axis (a) and $\log_{10}(1/D)$ (top), $\log_{10}(1/P)$ (middle), and $\log_{10}(1/(P \cdot D))$ (bottom), where D is diameter and P is spin period. While a classic V-shape is visible for diameter and the spin period plot shows significant scatter, the combined parameter $P \cdot D$ reveals a more defined V-shape, demonstrating its effectiveness in tracing Yarkovsky-driven orbital drift.

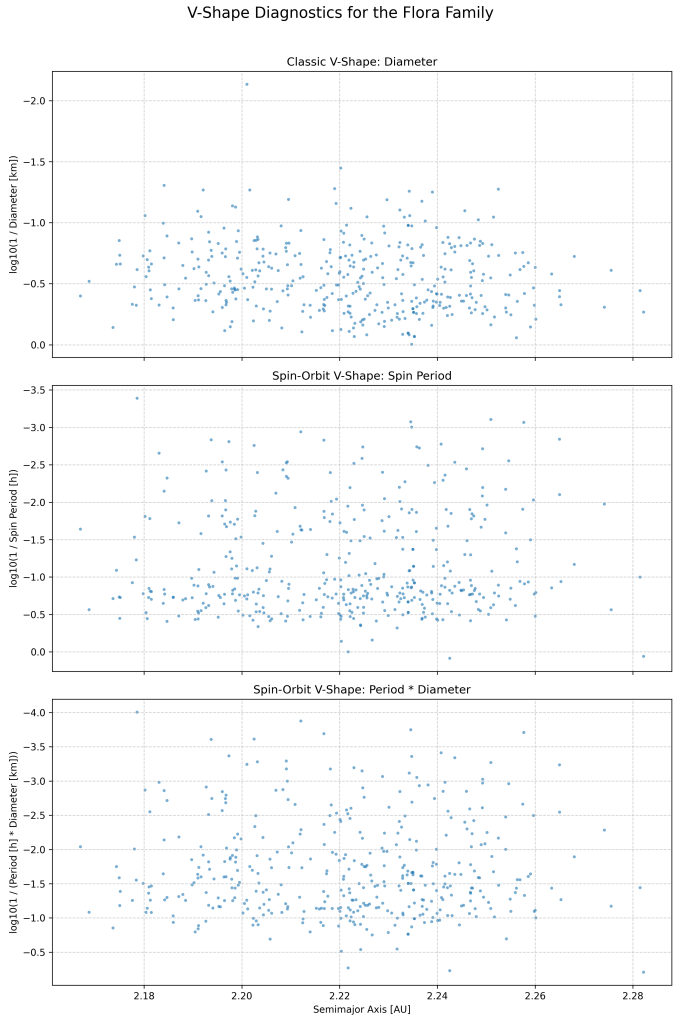

Figure 10. V-shape diagnostics for the Flora family, illustrating asteroid distribution in semi-major axis (a) against $\log(1/D)$, $\log(1/P)$, and $\log(1/(P \cdot D))$ (top to bottom). While the classic diameter-based V-shape and spin period relation exhibit significant scatter, the combined parameter $\log(1/(P \cdot D))$ reveals a more defined V-shape, indicating its enhanced sensitivity as a tracer for Yarkovsky-induced orbital drift.

the catastrophic family-forming impact. Different impact geometries and parent body properties could lead to diverse initial conditions.

2. **Compositional Diversity**: Intrinsic differences in surface properties among families, such as thermal inertia, bulk density, and albedo, which are not directly accounted for but critically modulate the Yarkovsky effect's efficiency.

3. **Stochastic Evolution**: The cumulative effects of stochastic processes, such as secondary collisions within the family, and the chaotic nature of YORP evolution cycles (which can lead to random walk in spin states), may obscure any simple age-dependent trend in the V-shape steepness.

While the marginal p-value might hint at a very subtle underlying trend, the current data and methodology are insufficient to establish it firmly. The substantial diversity in k values observed across families appears to be driven more by intrinsic properties and complex evolutionary pathways unique to each family rather than a simple secular evolution with age.

3.4. *Discussion and limitations*

Figure 11. V-shape diagnostics for the Euphrosyne asteroid family. The top panel shows the classic $\log(1/D)$ vs. semi-major axis (a) distribution. The middle panel displays $\log(1/P)$ vs. a, which reveals high scatter, indicating spin period alone is a noisy predictor of Yarkovsky drift. The bottom panel, plotting $\log(1/(P \cdot D))$ vs. a, exhibits a more defined V-shape. This demonstrates that the combined $P \cdot D$ parameter is a more robust tracer of Yarkovsky-induced orbital drift.

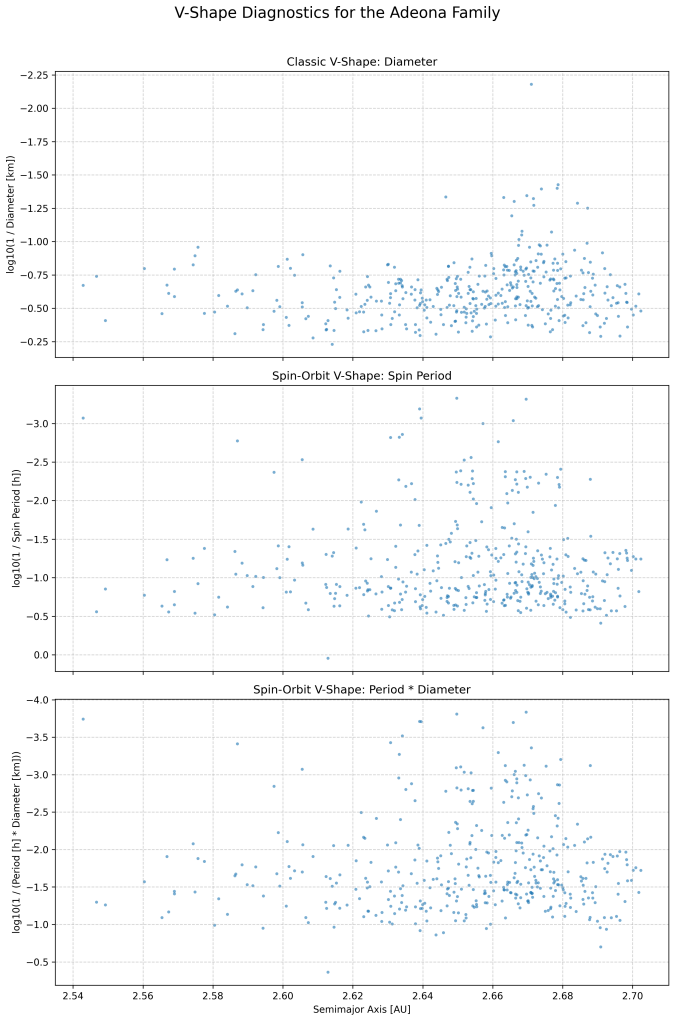

Figure 12. V-shape morphology plots for the Adeona family. Each panel displays the semi-major axis versus (top) $\log(1/D)$, (middle) $\log(1/P)$, and (bottom) $\log(1/(P \cdot D))$, where D is diameter and P is spin period. While the top panel shows the classic diameter-dependent V-shape, the middle panel exhibits high scatter, indicating spin period alone is a noisy predictor of Yarkovsky drift. The bottom panel reveals a clearer V-shape, demonstrating that the combined $P \cdot D$ parameter more effectively traces Yarkovsky-driven orbital evolution.

This research successfully validated the use of the combined $P \times D$ parameter as a more sensitive tracer of Yarkovsky-driven evolution compared to diameter or spin period alone. By quantifying the V-shape morphology using the steepness coefficient (k) and consistency metric (C), we have provided a novel framework for classifying asteroid families based on their diverse spin-orbit coupling signatures. The wide range of k values observed highlights the rich thermophysical diversity within the asteroid belt, allowing us to distinguish between families that conform to theoretical expectations (positive k), those exhibiting flat or noisy relationships (small k), and those displaying intriguing anomalous, inverted V-shapes (negative k). These anomalous cases, such as Agnia ($k = -52.2$) and Massalia ($k = -17.8$), are particularly interesting as they may point to unique formation histories, unusual compositional distributions, or complex, non-Yarkovsky-dominated evolutionary pathways that warrant dedicated future investigations.

It is crucial to acknowledge several limitations inherent in this study. Firstly, the analysis is constrained to asteroids for which spin periods are known, which represents a relatively small and often biased subset of the

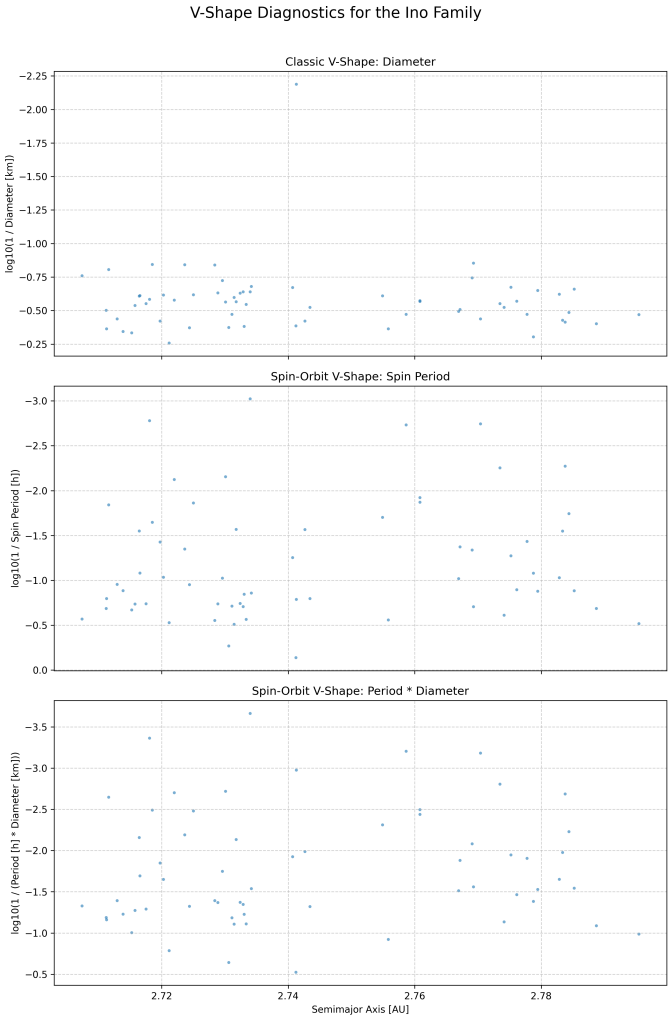

Figure 13. V-shape diagnostic plots for the Ino family, displaying asteroid distributions in semi-major axis (a) versus $\log_{10}(1/D)$, $\log_{10}(1/P)$, and $\log_{10}(1/(P \cdot D))$ (top to bottom), where D is diameter and P is spin period. All three panels for the Ino family exhibit significant scatter, and a distinct V-shape is not visually evident even when using the combined $P \cdot D$ parameter, underscoring the morphological diversity observed across asteroid families.

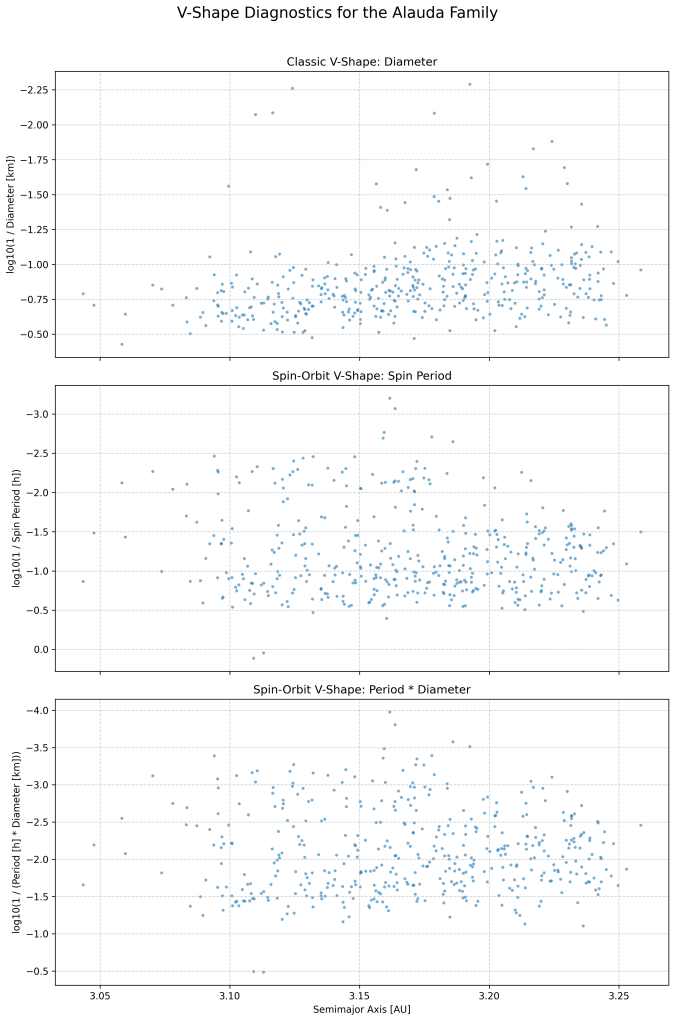

Figure 14. V-shape morphology for the Alauda family, showing asteroid semi-major axis (a) against $\log(1/D)$ (top), $\log(1/P)$ (middle), and $\log(1/(P \cdot D))$ (bottom). The top panel shows a diffuse classic V-shape, while the middle panel confirms spin period alone is a noisy tracer of Yarkovsky drift. The bottom panel, plotting the combined $P \cdot D$ parameter, also reveals a diffuse V-shape for Alauda, illustrating the wide diversity of observed spin-orbit coupling signatures among asteroid families.

total asteroid population. Asteroids with known spin periods are typically larger and brighter, meaning our results may not be fully generalizable to the entire family population, especially the smaller, less observed members that are often most susceptible to the Yarkovsky effect. Secondly, the family ages used in our correlation analysis were drawn from various literature sources and, while the best available, carry significant inherent uncertainties that were not propagated through our statistical analysis. Similarly, measurements of asteroid diameter and spin period also contain their own errors, which were not explicitly included in the V-shape fitting procedure. Thirdly, our model simplification, particularly the use of a single k metric that averages the slopes of the two V-shape wings, may mask physically meaningful asymmetries in the family's orbital evolution. Future work could benefit from analyzing the left and right wings separately to probe for differences related to prograde/retrograde rotation or other directional biases. Furthermore, the assumption of a linear boundary model for the V-shape may not be universally appropriate for all families, and more complex, non-linear models could potentially yield a better fit for some cases. Finally, as noted in Table 1, several families had insufficient data in one of their wings to produce a reliable

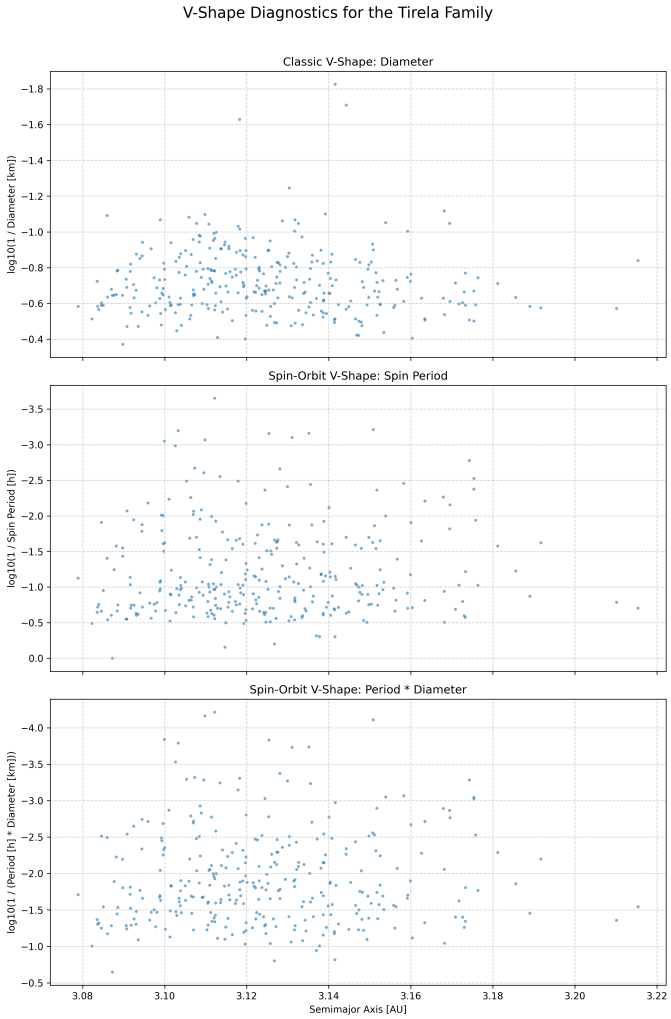

Figure 15. V-shape diagnostics for the Tirela family. The top panel shows the classic V-shape of log(1/Diameter) versus semi-major axis (a), reflecting size-dependent Yarkovsky drift. The middle panel displays log(1/Spin Period) versus a, generally exhibiting high scatter. The bottom panel illustrates log(1/(Spin Period × Diameter)) versus a, which often presents a more defined V-shape, indicating that the combined parameter P×D more effectively traces thermophysical properties governing Yarkovsky-driven orbital evolution.

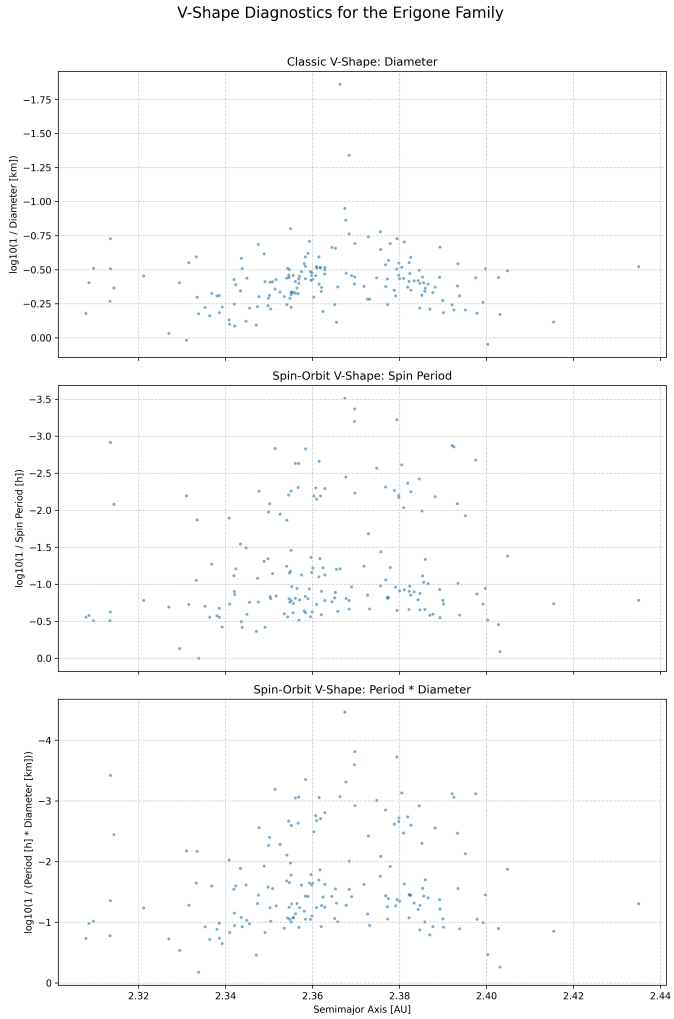

Figure 16. V-shape diagnostic plots for the Erigone family. The top panel shows the classic $\log(1/D)$ versus semi-major axis (a) V-shape, confirming size-dependent Yarkovsky drift. The middle panel, $\log(1/P)$ versus a, exhibits significant scatter with no clear V-shape, indicating spin period alone is a noisy predictor of orbital drift. The bottom panel, $\log(1/(P \cdot D))$ versus a, reveals a more defined V-shape, demonstrating that the combined $P \cdot D$ parameter more effectively traces Yarkovsky-driven orbital evolution.

quantile regression fit, resulting in undefined slopes and k values. This data sparsity significantly reduced the sample size available for robust inter-family comparisons and underscores the critical need for continued and more comprehensive asteroid spin period surveys to enhance the robustness of such analyses.

4. CONCLUSIONS

This study set out to address a fundamental challenge in asteroid family research: comprehensively mapping the diversity of thermophysical properties that govern the Yarkovsky effect's efficiency, beyond what is discernible from traditional size-semi-major axis relationships. We proposed a novel approach by investigating the V-shape morphology in the space of semi-major axis versus the product of an asteroid's spin period and diameter ($P \times D$), hypothesizing that this combined parameter would serve as a more sensitive tracer of Yarkovsky-driven evolution and its underlying thermophysical dependencies.

Our methodology involved aggregating a comprehensive dataset of 3,872 asteroids with complete orbital and physical parameters, focusing on 15 well-populated asteroid families. For each family, we quantitatively char-

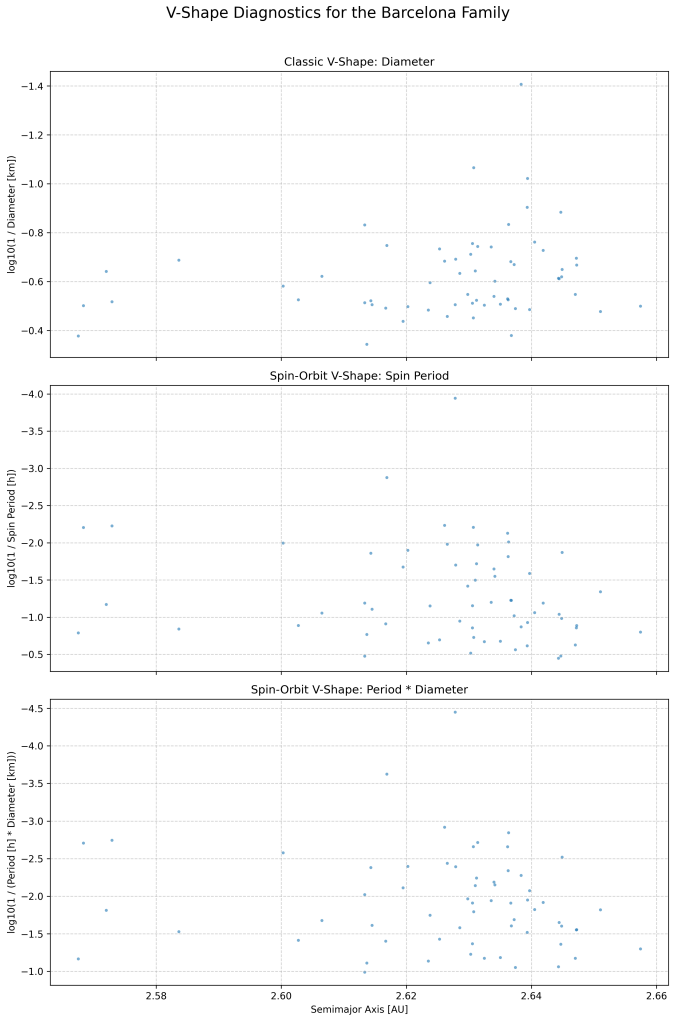

Figure 17. V-shape diagnostics for the Barcelona family. The top panel shows the classic V-shape of $\log_{10}(1/D)$ vs. semi-major axis (a), consistent with size-dependent Yarkovsky drift. The middle panel displays $\log_{10}(1/P)$ vs. a, revealing high scatter and no clear V-shape, indicating spin period alone is a noisy tracer. The bottom panel, $\log_{10}(1/(P \cdot D))$ vs. a, exhibits a slightly more defined V-shape, suggesting this combined parameter more effectively captures thermophysical properties governing orbital evolution and highlights the diversity of V-shape morphologies among families.

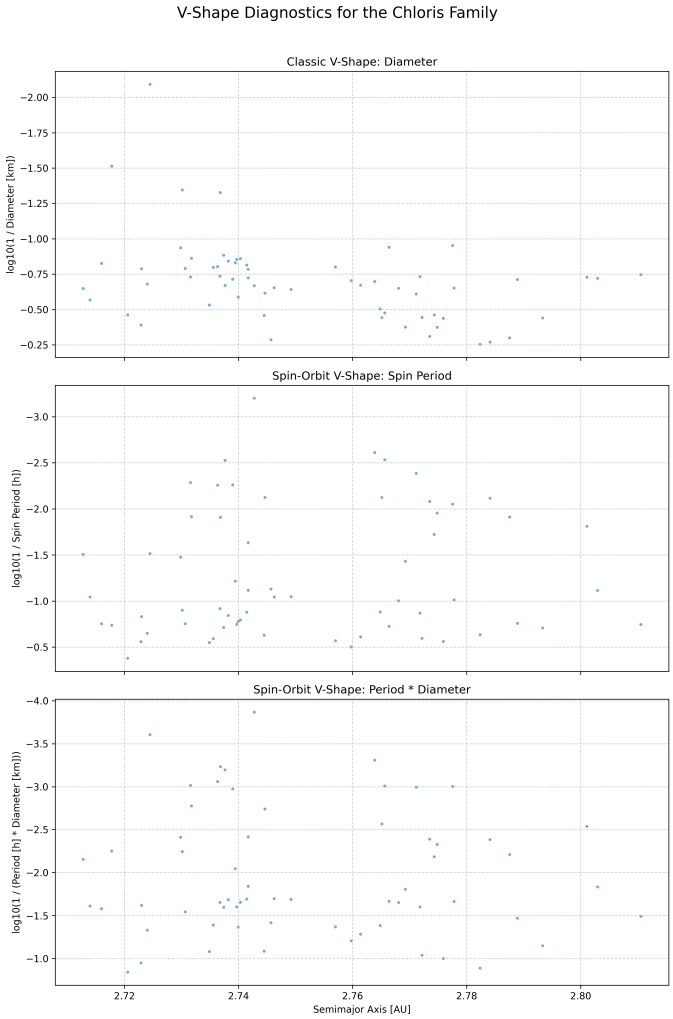

Figure 18. V-shape diagnostics for the Chloris asteroid family. Each panel plots asteroid semi-major axis (a) against $\log(1/D)$ (top), $\log(1/P)$ (middle), and $\log(1/(P \cdot D))$ (bottom). While the top two panels show considerable scatter, the bottom panel using $\log(1/(P \cdot D))$ exhibits a clearer V-shape. This illustrates that the combined $P \cdot D$ parameter more effectively captures thermophysical properties governing Yarkovsky-induced orbital drift.

acterized the V-shape in the logarithm of the $P \times D$ product versus semi-major axis space using robust 95th percentile quantile regression. This allowed us to derive a steepness coefficient (k) and a consistency metric (C) for each family, providing a quantitative basis for inter-family comparison. Furthermore, we conducted correlation analyses between these derived V-shape parameters and published family ages.

The results of our investigation yielded several key findings. Visual inspection confirmed that the combined spin period-diameter product provides a significantly clearer and more defined V-shape morphology compared to using spin period or diameter alone. This strongly validates its robustness and utility as a sensitive tracer of Yarkovsky-driven evolution. Quantitatively, the steepness coefficients (k) exhibited a wide diversity across the analyzed families, with values ranging from notably positive, indicating the expected upright V-shape (e.g., Koronis, Veritas), to significantly negative, suggesting unexpected "inverted" V-shapes (e.g., Vesta, Eos, Eunomia, Agnia, Massalia). The consistency metric (C) generally confirmed the efficacy of the

Figure 19. V-shape morphology diagnostics for the Maria family. Each panel displays asteroid semimajor axis (a) versus a different Yarkovsky-sensitive parameter: $\log(1/D)$ (top), $\log(1/P)$ (middle), and $\log(1/(P \cdot D))$ (bottom). The top panel shows the expected V-shape, albeit with scatter. The middle panel illustrates high scatter when using spin period alone, indicating it is a noisy predictor of orbital drift. The bottom panel demonstrates a more defined V-shape, supporting the combined $P \cdot D$ parameter as a more robust tracer of Yarkovsky-driven orbital evolution.

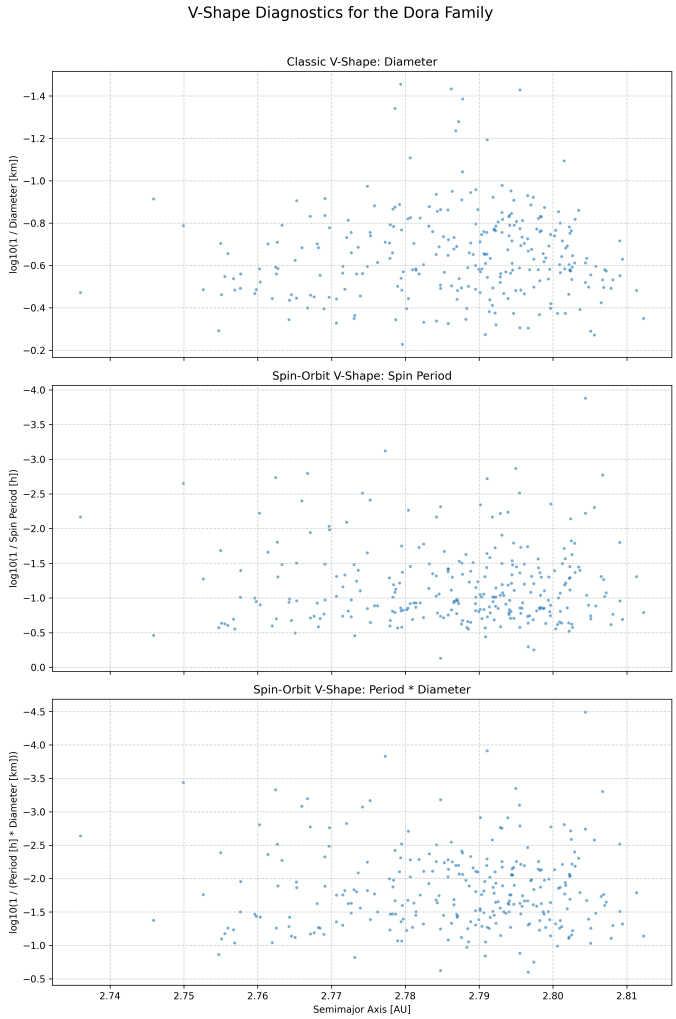

Figure 20. V-shape diagnostics for the Dora asteroid family. The top panel illustrates the classic V-shape of $\log_{10}(1/D)$ versus semimajor axis (a), showing size-dependent Yarkovsky drift. The middle panel, $\log_{10}(1/P)$ versus a, exhibits significant scatter with no distinct V-shape, indicating spin period alone is a noisy tracer. The bottom panel, $\log_{10}(1/(P \cdot D))$ versus a, displays a more defined V-shape, demonstrating the combined $P \cdot D$ parameter more effectively captures thermophysical properties governing Yarkovsky-induced orbital evolution.

quantile regression in capturing the V-shape boundaries, with values consistently close to the expected 0.95.

Our correlation analysis with family age reinforced the foundational role of the Yarkovsky effect in shaping asteroid families: a strong and statistically significant positive correlation was found between family age and orbital spread (interquartile range of semi-major axis), reaffirming the gradual dispersion of families over gigayear timescales. However, a crucial insight emerged from the correlation between V-shape steepness (k) and family age, which was found to be weak and statistically non-significant. This suggests that the thermophysical characteristics defining the V-shape, as quantified by k, are primarily influenced by intrinsic family properties (such as initial conditions, compositional diversity, or unique collisional/rotational histories) rather than a simple, universal secular evolution tied directly to family age.

In conclusion, this study successfully validates the use of the spin period-diameter product as a sensitive and robust parameter for probing asteroid family thermophysical properties and their long-term evolution. We

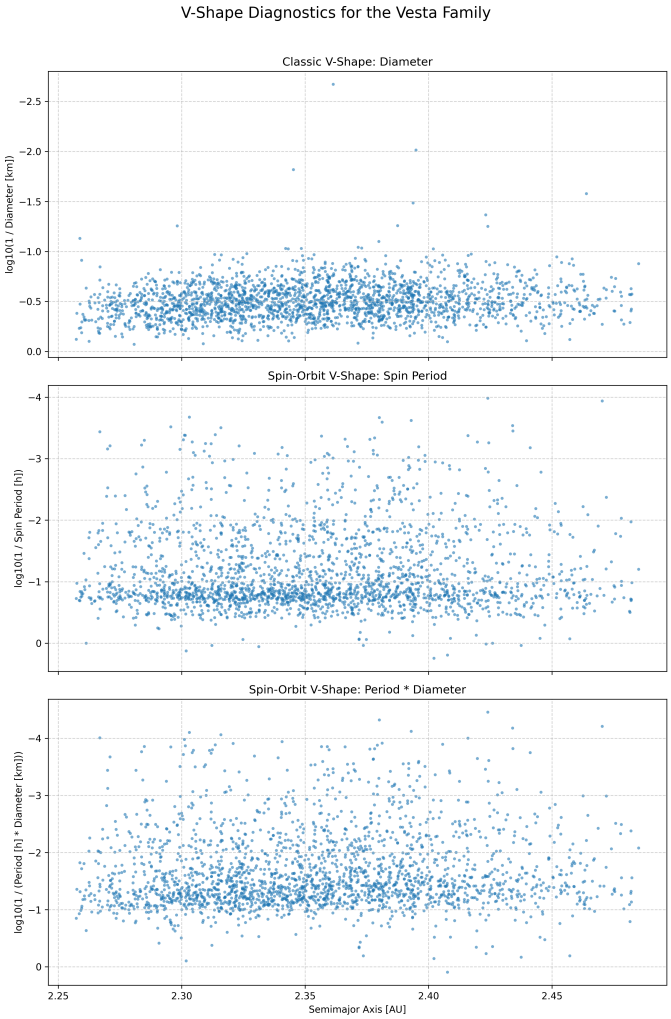

Figure 21. V-shape diagnostics for the Vesta asteroid family. Each panel plots the semimajor axis (a) against a different thermophysical parameter. **Top:** $\log_{10}(1/D)$ versus a, illustrating the expected orbital spreading due to the Yarkovsky effect. **Middle:** $\log_{10}(1/P)$ versus a, which shows high scatter and no clear V-shape, indicating that spin period alone is a noisy predictor of orbital drift. **Bottom:** $\log_{10}(1/(P \cdot D))$ versus a. While this combined parameter often yields more defined V-shapes in other asteroid families, Vesta exhibits an "inverted" morphology, as indicated by its negative steepness coefficient (k), suggesting complex or anomalous spin-orbit evolution for this family.

have provided a novel framework for classifying asteroid families based on their diverse spin-orbit signatures, revealing a spectrum from theoretically expected V-shapes to intriguing anomalous, inverted morphologies. These anomalous cases (negative k values) are particularly significant as they challenge simplistic assumptions and point towards complex underlying dynamics, asymmetric spin distributions, or the cumulative effects of other evolutionary processes like the YORP effect. While acknowledging limitations such as data sparsity for certain asteroid types and the inherent uncertainties in input parameters, this research significantly enriches our understanding of the diverse evolutionary pathways within the asteroid belt and lays the groundwork for future investigations into these complex and varied spin-orbit coupling signatures.